

# 000 001 002 003 004 005 006 007 008 009 010 011 012 013 014 015 016 017 018 019 020 021 022 023 024 025 026 027 028 029 030 031 032 033 034 035 036 037 038 039 040 041 042 043 044 045 046 047 048 049 050 051 052 053 BIOVERSE: REPRESENTATION ALIGNMENT OF BIOMEDICAL MODALITIES TO LLMS FOR MULTI- MODAL REASONING

Anonymous authors

Paper under double-blind review

## ABSTRACT

Recent advances in large language models (LLMs) and biomedical foundation models (BioFMs) have achieved strong results in biological text reasoning, molecular modeling, and single-cell analysis, yet they remain siloed in disjoint embedding spaces, limiting cross-modal reasoning. We present BIOVERSE (**B**iomedical **V**ector **E**mbedding **R**ealignment for **S**emantic **E**ngagement), a two-stage approach that adapts pretrained BioFMs as modality encoders and aligns them with LLMs through lightweight, modality-specific projection layers. The approach first aligns each modality to a shared LLM space through independently trained projections, allowing them to interoperate naturally, and then applies standard instruction tuning with multi-modal data to bring them together for downstream reasoning. By unifying raw biomedical data with knowledge embedded in LLMs, the approach enables zero-shot annotation, cross-modal question answering, and interactive, explainable dialogue. Across tasks spanning cell-type annotation, molecular description, and protein function reasoning, compact BIOVERSE configurations surpass larger LLM baselines while enabling richer, generative outputs than existing BioFMs, establishing a foundation for principled multi-modal biomedical reasoning.

## 1 INTRODUCTION

High-throughput assays such as scRNA-seq, proteomics, and small-molecules profiling generate rich, high-dimensional data that are critical for biomedical discovery. Biomedical foundation models (BioFMs; also referred to as BMFMs) trained on those inputs, e.g., scGPT (Cui et al., 2024) for single-cell RNA sequencing (scRNA-seq), ESM-2 (Lin et al., 2023) for proteins, Molformer (Ross et al., 2022) for small molecules, capture expressive representations but lack instruction-following and open-ended reasoning. In contrast, general-purpose large language models (LLMs) excel at language interaction and can nominally ingest sequences like proteins or Simplified Molecular Input Line Entry System (SMILES) strings, but tokenization yields short, uninformative fragments and they cannot parse modalities such as scRNA-seq, where a cell’s gene expression vector cannot be represented meaningfully as a token sequence. Bridging these strengths requires a framework that preserves modality-specific encoders, aligns their embeddings with the LLM token space, and enables reasoning across them.

We introduce BIOVERSE, a framework adapting the familiar vision–language paradigm (e.g., Flamingo (Alayrac et al., 2022), BLIP-2 (Li et al., 2023), LLaVA (Liu et al., 2023a)), and more recently, InternVL3.5 (Wang et al., 2025b), to the biomedical domain. BIOVERSE follows a BioFM-adapter-LLM design: it projects BioFM embeddings into the LLM’s embedding space via a lightweight MLP adapter and injects them as special tokens (e.g. [BIO\_1], [BIO\_2], ..., [BIO\_k], and [TRAINABLE\_BIO]). By placing biological and textual information in a shared space, BIOVERSE enables joint multi-modal reasoning while directly exploiting the LLM’s native memory and inference abilities. Our contributions are:

- **Modular architecture:** Plug-and-play biological encoders (scRNA-seq, protein, molecule) connect to a decoder-only LLM via a small projection layer and LoRA adapters.
- **Alignment via contrastive learning:** We directly align encoder embeddings to the language token space, i.e., no separate bio-language encoder, enabling zero-shot transfer across modalities.

- **Multimodal instruction tuning:** We curate paired (embedding, instruction, response) data so the LLM learns to use biological context in generation.
- **Practicality:** Compact BIOVERSE variants match or exceed larger baselines on joint bio–text tasks and support privacy-preserving, on-prem deployments. This aligns with the current trend of promoting small language models in the agentic AI systems (Belcak et al., 2025).

## 2 RELATED WORK

**Biomedical encoders.** Large-scale BioFMs have been developed for modality-specific data. For transcriptomics, models such as scBERT (Yang et al., 2022), Geneformer (Theodoris et al., 2023), and scGPT (Cui et al., 2024) capture cellular states and gene–gene dependencies, with BMFM-RNA (Dandala et al., 2025) providing a reproducible framework for pretraining. For proteins, ProteinBERT (Brandes et al., 2022) and ESM-2 (Lin et al., 2023) learn contextual embeddings that support function and family prediction, while AlphaFold (Jumper et al., 2021) and ESMFold (Lin et al., 2023) show how such embeddings enable structure prediction. In the molecular domain, ChemBERTa (Chithrananda et al., 2020) and MolFormer (Ross et al., 2022) encode SMILES strings and molecular graphs into embeddings of chemical properties. Together, these unimodal encoders yield strong representations but lack natural-language reasoning.

**Bio-LLM integration.** Several efforts have explored bridging biological embeddings with language models; however, current methods only partially address the challenge of joint bio–text reasoning. GenePT (Chen & Zou, 2024) pools gene-level embeddings derived from ChatGPT descriptions into cell-level representations, which work well for classification but are not integrated into an LLM’s generation pipeline. CELLama (Choi et al., 2024) prompts LLMs with transcriptomic profiles converted into text-like inputs. While effective for flexible queries, it does not exploit pretrained BioFMs trained directly on raw scientific data, limiting its ability to capture domain-specific signal. scCello (Yuan et al., 2024) and scMulan (Bian et al., 2024) incorporate text labels or metadata as supervision to improve biological embeddings, but the resulting embeddings remain modality-specific and are not aligned with text embeddings from LLMs, limiting their use for joint bio–text reasoning. CellWhisperer (Schaefer et al., 2024) uses Geneformer (Theodoris et al., 2023) and BioBERT (Lee et al., 2020) to align scRNA-seq and text embeddings. While this enables retrieval, differences in tokenization and architecture prevent seamless integration with generative LLMs, leading to a RAG-style pipeline rather than embedding-aware reasoning. TxGemma (Wang et al., 2025a), BioT5 (Pei et al., 2023), and Galactica (Taylor et al., 2022) fine-tune general-purpose or biomedical LLMs on biological sequences tokenized as text (e.g., amino acids, SMILES, or curated biomedical corpora). This design enables strong domain-specific reasoning and therapeutic applications but constrains the models to operate entirely in the text-token space. As a result, they do not leverage pretrained BioFMs trained on raw molecular or cellular data, limiting their ability to capture low-level biological signals and reducing extensibility across modalities. MAMMAL (Shoshan et al., 2024) unifies multiple bio-modalities and supports generation in a T5-style foundation model trained end-to-end on diverse data, but its monolithic nature and custom tokenizer preclude modular embedding reuse or deployment within modern instruction-tuned LLMs.

**General multi-modal LLMs.** In the general AI domain, vision-language models demonstrate how non-text modalities can be modularly aligned with LLMs. Approaches like LLaVA, BLIP-2, Flamingo, and more recently InternVL 3.5 (Liu et al., 2023a; Li et al., 2023; Alayrac et al., 2022; Wang et al., 2025b) established a design pattern where modality-specific encoders are efficiently connected to LLMs through projection and instruction tuning. This pattern has yet to be fully realized in biomedicine, where biological and text embeddings remain misaligned.

**Positioning of BIOVERSE.** Building on the proven encoder-projector-LLM design pattern from vision-language models, BIOVERSE addresses the gap between biological and textual embedding spaces by projecting BioFM outputs directly into the LLM’s input embedding space. This modular alignment enables pretrained encoders for scRNA-seq, proteins, or molecules to be integrated without retraining the LLM. By treating these embeddings as first-class tokens, BIOVERSE allows the model to reason jointly over biological data and natural language, providing a flexible foundation for cross-modal biomedical intelligence.

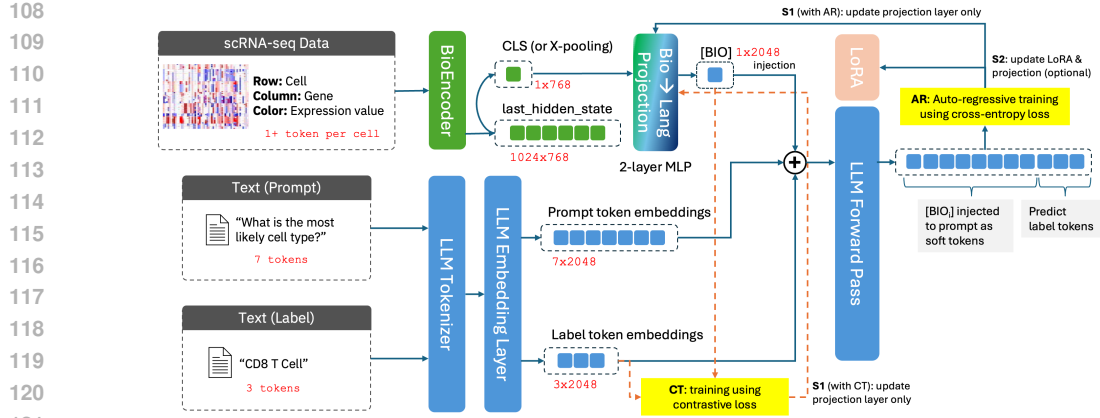


Figure 1: BIOVERSE base architecture: a modality-specific BioFM encodes a biological entity, and its output embeddings are mapped by a projection layer into the LLM’s embedding space via special tokens (e.g. [BIO]). In the alignment stage, only the projection layer  $P_\theta$  is trainable, while the encoder  $f_b$  and the LLM  $g$  remain frozen. In the subsequent instruction-tuning stage, we allow both  $P_\theta$  and the low-rank adapter (LoRA) within the LLM to be trainable. Stage 1 (S1) can be trained using autoregressive (AR) or contrastive (CT) loss, while stage 2 (S2) is always AR.

### 3 METHOD

#### 3.1 PROBLEM SETUP

Given a biological input  $x_b$  (e.g., a protein sequence or an scRNA-seq profile) and a natural-language context or query  $q$ , our goal is to enable a frozen LLM to jointly reason over  $(x_b, q)$ . We use a pretrained BioFM  $f_b$  to encode  $x_b$  into one or more embeddings  $z_b$ , and a lightweight projection  $P_\theta$  to map  $z_b$  to the LLM’s token-embedding space. These projected embeddings are injected at designated marker positions, e.g., [BIO], and act as soft tokens that the frozen decoder can attend to. The key challenge is that bio embeddings and text embeddings are trained in siloed spaces and must be aligned for effective joint reasoning.

#### 3.2 TWO-STAGE TRAINING

**Alignment** Although LLM can, in principle, learn cross-space attention through sufficient instruction tuning, pre-aligning the bio and language embeddings provides a strong inductive prior: it reduces task-specific tuning burden and improves zero/few-shot generalization to unseen tasks. To achieve this, we introduce a CLIP-style alignment stage using paired data  $(x_b, t_b)$ , where the projection  $P_\theta$  is trained so that the bio embedding  $z_b = f_b(x_b)$  is close to its language counterpart  $\phi(t_b)$ , which represents the text’s embedding.

In the base training mode illustrated in Figure 1, all data is processed through LLM’s forward pass, and a standard autoregressive cross-entropy loss (with teacher forcing) is used to guide learning. Alternatively, to avoid the costly forward pass required by a large LLM, and to enable alignment with efficient encoder models that are often co-trained with the decoder for retrieval, we evaluate an alternative alignment mode. In this variant, we use contrastive learning to directly align the bio embeddings with their paired text embeddings. From here onward, we denote the first alignment strategy as AR (autoregressive) and the second as CT (contrastive).

**Instruction Tuning** The alignment stage maps BioFM embeddings into the LLM’s token space; the instruction tuning stage teaches the decoder to use those soft tokens under real prompts, improving generative reasoning, prompt robustness, and likelihood calibration. Abundant curated corpora (e.g., TxGemma-processed instruction sets and Therapeutics Data Commons (TDC) tasks) can be readily adapted for multi-task SFT, making this step practical with minimal data engineering. However, instruction tuning can confound alignment comparisons, increase compute and hyperparameter burden, and cause geometry drift. Given that our focus is alignment, we do not perform extensive instruction tuning.

162 3.3 MODULAR ARCHITECTURE  
163164 **Biological Encoder** We use a pretrained BioFM  $f_b : \mathcal{X}_b \rightarrow \mathbb{R}^{k \times d_b}$  to encode a biological input  $x_b$   
165 into  $k$  embeddings:<sup>1</sup>

166 
$$z_b = f_b(x_b), \quad z_b \in \mathbb{R}^{k \times d_b}$$

167 Any BioFM appropriate to the modality can be used, provided a bio embedding can be extracted  
168 from its output or an intermediate layer. We refer to it as an encoder to highlight its role in mapping a  
169 biological entity into an embedding, although the underlying architecture may be an encoder or a  
170 decoder. Some BioFMs return a single pooled embedding (e.g., scGPT (Cui et al., 2024), scBERT  
171 (Yang et al., 2022)), while others output a sequence of contextual embeddings (e.g., per-residue  
172 embeddings in ESM-2 (Lin et al., 2023), or per-token embeddings over SMILES in ChemBERTa  
173 (Chithrananda et al., 2020)). In practice, these sequence outputs are often pooled to obtain a single  
174 vector per entity, but our framework supports both pooled and multi-token cases.175 **Projection Layer** The projection  $P_\theta : \mathbb{R}^{d_b} \rightarrow \mathbb{R}^{d_t}$  is a lightweight MLP with ReLU activations,  
176 layer normalization, and dropout for stability. It maps the BioFM output into the LLM embedding  
177 space:

178 
$$\tilde{z}_b = P_\theta(z_b), \quad \tilde{z}_b \in \mathbb{R}^{k \times d_t}$$

179 In vision-language models, tens to hundreds of tokens are used per image (e.g., BLIP-2 (Li et al.,  
180 2023), CLIP (Radford et al., 2021)), often requiring token-level normalization or gating for stability.  
181 By contrast, BioFMs usually pool to a single token, reflecting that cells, proteins, and molecules are  
182 typically treated as indivisible units, and a lightweight projection is sufficient to ensure compatibility  
183 with the LLM while preserving BioFM semantics.184 **Injection of Bio Tokens** We inject the projected bio embeddings  $\tilde{z}_b$  at a placeholder (e.g., [BIO])  
185 within the query  $q$ , replacing the marker with the embeddings as soft tokens before concatenating  
186 with the rest of the sequence:

187 
$$[\text{Tokens}(q, [\text{BIO}] \rightarrow \tilde{z}_b) ; \text{Tokens}(t_b)].$$

188 Here,  $\text{Tokens}(\cdot)$  denotes text after tokenization and embedding lookup. While standard text inputs are  
189 mapped from token IDs through the embedding matrix, projected bio embeddings are fed directly into  
190 the LLM embedding layer (via the `inputs_embeds` interface in many implementations), enabling  
191 integration without modifying the tokenizer or embedding matrix.192 **Language Embedding Targets** When performing alignment training using AR loss, the model  
193 consumes  $\text{Tokens}(t_b)$  directly, since the objective is next-token prediction over a text sequence.  
194 However, to also support CT loss that enforces representation-level similarity, we require a single  
195 pooled representation of the text. We therefore define a frozen language embedding  $\phi(t_b) \in \mathbb{R}^{d_t}$   
196 extracted from the target LLM. Choices of the target will be discussed later in detail.197 **Language Model** We extend a small LLM  $g$  with a few soft tokens, without modifying its tokenizer  
198 or positional encodings. As the lightweight projection layer decoupled the LLM and requires only  
199 embedding dimension compatibility, our approach can directly scalable to larger LLMs.200 3.4 ALIGNMENT OBJECTIVES  
201202 **Autoregressive Decodability.** Our default alignment strategy is to directly train the LLM to use  
203 the projected bio embeddings during generation. Given a query  $q$ , bio embeddings  $\tilde{z}_b$  injected at a  
204 [BIO] marker, and paired target text  $t_b = (t_1, \dots, t_{|t_b|})$ , we minimize the negative log-likelihood of  
205 predicting  $t$  in an autoregressive manner:

206 
$$\mathcal{L}_{\text{AR}} = - \sum_{i=1}^{|t_b|} \log p_{\text{LLM}}(t_i | \tilde{z}_b, q, t_{<i})$$

207 This objective explicitly teaches the LLM to attend to bio tokens in the same way it attends to text  
208 tokens, ensuring decodability and downstream reasoning ability. Because the loss is defined over  
209 natural text generation, it tightly couples alignment with the LLM’s causal decoding process.210 <sup>1</sup>For notational simplicity, we assume  $k = 1$  and omit the token index in most equations from here onward;  
211 the framework naturally extends to  $k > 1$  when multiple embeddings are injected

**Contrastive Alignment.** In addition to autoregressive decodability, we also study a contrastive alignment mode that enforces representation-level similarity. Here, the projected bio embeddings  $\tilde{z}_b$  are aligned with text embeddings  $\phi(t_b)$  from paired descriptions using a bidirectional InfoNCE loss:

$$\mathcal{L}_{\text{CT}} = -\frac{1}{2N} \sum_{i=1}^N \left[ \underbrace{\log \frac{\exp(\text{sim}(\tilde{z}_b^{(i)}, \phi(t_b^{(i)}))/\tau)}{\sum_{j=1}^N \exp(\text{sim}(\tilde{z}_b^{(i)}, \phi(t_b^{(j)}))/\tau)}}_{\text{bio} \rightarrow \text{text}} + \underbrace{\log \frac{\exp(\text{sim}(\phi(t_b^{(i)}), \tilde{z}_b^{(i)})/\tau)}{\sum_{j=1}^N \exp(\text{sim}(\phi(t_b^{(i)}), \tilde{z}_b^{(j)})/\tau)}}_{\text{text} \rightarrow \text{bio}} \right]$$

where  $\text{sim}(\cdot, \cdot)$  denotes cosine similarity and  $\tau$  is a learnable temperature. Note that the denominator from bio to text normalizes over all text embeddings, and the denominator from text to bio normalizes over all bio embeddings. Prior work (e.g. CLIP (Radford et al., 2021), BLIP-2 (Li et al., 2023)) shows including both directions stabilizes training.

We explore contrastive alignment for three main reasons: (1) it enforces semantic consistency between bio and text embeddings rather than relying solely on next-token prediction, which may improve generalization to unseen tasks; (2) it decouples alignment from the frozen LLM decoder, allowing alternative text encoders to serve as alignment targets; and (3) it is computationally efficient, bypassing the LLM’s forward pass to directly align paired  $(x_b, t_b)$  examples. An additional benefit, observed in prior work, is that contrastive objectives produce more isotropic embedding spaces and can exploit large in-batch negatives, improving transfer and data efficiency.

## 4 EXPERIMENTAL SETUP

### 4.1 MODELS

**Biological Encoder** We evaluate representative foundation models across three modalities (all pooled into a single embedding at the end): scGPT (Cui et al., 2024) for scRNA-seq, ESM-2 (Lin et al., 2023) for proteins, and ChemBERTa (Chithrananda et al., 2020) for small molecules. We also include MAMMAL (Shoshan et al., 2024), a multimodal biomedical model that supports all three modalities. Finally, we consider a general-domain LLM used directly as a bio encoder. Although LLMs can ingest serialized versions of biological entities (e.g., scRNA-seq approximated by sorting genes into a sequence, while proteins and SMILES strings are natively sequential), the resulting tokenizations tend to be short and poorly contextualized, and we suspect it limits biological fidelity.

**Language Model** We evaluate two scales of LLMs as the language backbone. As a small model, we use Granite-3.3-8B-Instruct (Granite-8B for short), an 8B open-weights model released by IBM Research, to demonstrate alignment effectiveness under limited capacity. BIOVERSE is LLM-agnostic: any model that accepts embedding inputs (as is the case for most HuggingFace LLMs) can be used without architectural changes.<sup>2</sup> For comparison against large-scale baselines that do not leverage BioFMs for encoding, we also evaluate GPT-OSS-120B, a public 120B open-weights model by OpenAI, details of models see App. A.2)..

**Projection Layer** The projection is implemented as a three-layer MLP with ReLU activations, layer normalization, and dropout for stability.

**Language Embedding Target** We evaluate four ways to construct  $\phi(t)$ : (1) **TokEmbed**, averaging input embeddings; (2) **LL-Mean**, mean pooling of the final layer; (3) **LayerAvg**, averaging several top layers; and (4) **LLM-Embed**, a co-trained text encoder when available. TokEmbed performed poorly, and we adopt LL-Mean as the default. LLM-Embed shows strong results but applies only under contrastive training; systematic study of LayerAvg and LLM-Embed is left for future work.

### 4.2 DATASETS AND EVALUATION

#### 4.2.1 ALIGNMENT

For alignment, we construct paired biological entities  $(x_b)$  and textual descriptions  $(t_b)$  across three modalities. **Protein:** We obtain protein–text pairs from UniProtKB, where each amino acid sequence

<sup>2</sup>In practice, this requires only that the LLM expose an `inputs_embeds` interface or equivalent.

270 is linked to curated Gene Ontology (GO) terms representing its functional annotations across the  
 271 three GO namespaces: Biological Process, Molecular Function, and Cellular Component. GO term  
 272 metadata is derived from the official GO ontology, and annotations are obtained from UniProt cross-  
 273 references. To ensure reliability, we retain only experimentally supported GO annotations, yielding  
 274 high-quality supervision for aligning BioFM protein embeddings with language representations.  
 275 **Small Molecule:** For small molecules, we leverage LLASmol (Yu et al., 2024), which provides  
 276 SMILES–text pairs with chemically grounded descriptions. Specifically, we select two datasets  
 277 from the LLASmol collection for BioFM alignment: SMILES-to-IUPAC conversion and molecule  
 278 captioning. In both cases, each molecule is represented as a SMILES string paired with natural-  
 279 language annotations of structure, properties, or activities. **scRNA-seq:** For single-cell data, we adopt  
 280 CellWhisperer (Schaefer et al., 2024), which aligns scRNA-seq profiles with cell-type and tissue-level  
 281 textual metadata. Following the dataset protocol, we use the CellxGene subset (Perkel, 2024), where  
 282 pseudo-bulk RNA samples are generated by averaging single-cell profiles, and natural-language  
 283 descriptions are produced from cell and tissue metadata using large language models. This enables  
 284 alignment between transcriptomic embeddings and ontological descriptions.

#### 285 4.2.2 INSTRUCTION TUNING

286 For Stage 2 instruction tuning, we augment the alignment dataset with templated prompts paired to  
 287 the biological–text examples. This teaches the LLM to use aligned bio tokens under user queries;  
 288 for example, “*What cell type matches this [BIO]gene-expression profile?*” Since the primary  
 289 goal of this paper is to evaluate architectural design rather than extensive prompt handling, we limit  
 290 instruction tuning to light augmentation. This procedure can be readily extended with training data  
 291 from prior works such as TxGemma (Wang et al., 2025a), which introduces instruction-style data  
 292 for therapeutic reasoning tasks using the Therapeutics Data Commons (TDC), and CellWhisperer  
 293 (Schaefer et al., 2024) for cell-related tasks.

#### 295 4.3 EVALUATION

296 We evaluate our approach on six downstream tasks: five from Mol-Instruct (Fang et al., 2023)  
 297 (four protein-related and one small-molecule) and one from scEval (Liu et al., 2023b) (cell-type  
 298 annotation). Mol-Instruct provides molecular question–answer pairs spanning property prediction,  
 299 reaction reasoning, and therapeutic relevance, while scEval offers benchmarks for scRNA-seq  
 300 applications. For generative tasks, we report results using three complementary metrics. **LLM-as-  
 301 a-judge:** GPT-OSS-120B scores each model response independently against the expected output  
 302 with single-output, reference-based prompt (see Appendix A.4, repeating each evaluation three times  
 303 under different random seeds. **BERTScore:** captures semantic similarity. **ROUGE-L:** measures  
 304 surface-form overlap. Full definitions of the metrics and the prompt used for LLM-as-a-judge are  
 305 provided in Appendix A.1. Training details (learning rate, batch size, optimizer, training duration,  
 306 and compute resources) are documented in Appendix A.3.

## 308 5 RESULTS

### 311 5.1 EMBEDDING ALIGNMENT VISUALIZATION

312 To illustrate the effect of our alignment procedure, we present UMAP projections of scRNA-seq em-  
 313 beddings and their corresponding natural language embeddings before and after applying BioVERSE  
 314 alignment. As shown in Figure 2, prior to alignment, the two modalities occupy largely disjoint  
 315 regions of the latent space, whereas after training the projection layer they exhibit clear overlap,  
 316 indicating successful cross-modal alignment. These visualizations serve as a qualitative preview of  
 317 BioVERSE’s capacity to unify biological and textual representations.

### 319 5.2 MAIN RESULTS

#### 321 5.2.1 ZERO-SHOT GENERATIVE CELL TYPE ANNOTATION

322 We evaluate BioVERSE’s against two baselines on the PBMC10K dataset as discussed in scvi-tools  
 323 (Gayoso et al., 2022) under zero-shot generation: (1) random and majority baseline (2) open-domain

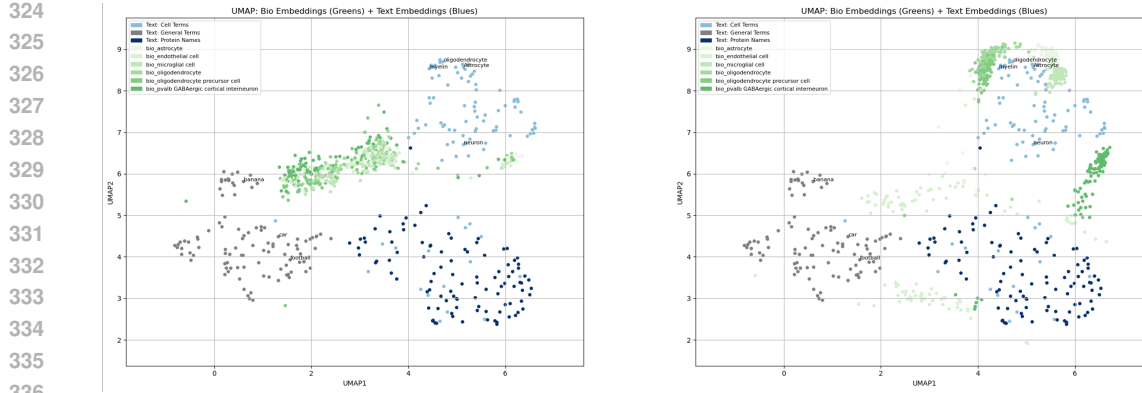


Figure 2: UMAP visualization of scRNA-seq and text embeddings. Left: before alignment, cell embeddings (green) form isolated clusters within the LLM embedding space. Right: after alignment, cell embeddings are pulled closer to biologically relevant text and separated from unrelated general-domain text. BIOVERSE successfully realigns the modalities into a shared representation space.

Table 1: Zero-shot PBMC10K results with 9 cell types.

	Baseline		Matching	Generative		
	Random	Majority	LangCell	Granite-8B	GPT-OSS-120B	BIOVERSE
Accuracy	0.111	0.417	0.865	0.369	0.779	0.614
Macro $F_1$	0.086	0.065	0.896	0.262	0.543	0.437

LLMs given a list of the 128 most expressed genes (sorted by expression count) as input. Alignment is trained on CellxGene data aggregated into pseudo-bulk samples as in CellWhisperer (Schaefer et al., 2024). The PBMC10K dataset used for evaluation is not present in CellxGene; however, CellxGene contains another PBMC dataset among its 1,800+ scRNA-seq datasets. Thus, while the exact test set is excluded, the ontology of cell types is shared. This reflects a realistic zero-shot transfer setting.

As shown in Table 1, although majority voting achieves relatively high accuracy, it fails on minority classes, leading to poor macro- $F_1$ . Prior BioFMs such as scGPT (Cui et al., 2024) and alignment-based models like LangCell (Zhao et al., 2024) and scMMGPT (Shi et al., 2025), when performing cell type annotation under zero-shot setting, fundamentally operate in a candidate-space matching paradigm. These models project cells and a predefined set of candidate labels and their descriptions into a shared embedding space and assign the nearest match. LangCell achieves the highest scores, reflecting the relative ease of candidate-space matching. By contrast, generative models operate in a generative regime: the LLM must produce a natural language label rather than selecting the nearest candidate. In our setup, we apply prompt-level constraints, instructing the model to select only from a predefined option set without decoding-level enforcement. The model nevertheless engages in open-ended reasoning before aligning to a candidate, making the task inherently more difficult. This setting, however, offers unique advantages: the ability to articulate rationales, propose novel labels outside a fixed ontology, and integrate bio-embeddings with broader biomedical knowledge.

Open-domain LLMs perform substantially better than chance, indicating that even with only sorted gene lists, LLMs show some inherent capability for this task. BIOVERSE improves substantially over its backbone (Granite-8B) while preserving and enhancing the LLM’s reasoning ability when both [BIO] and gene-list evidence are provided in the prompt. The [BIO] token guides the model toward the correct type, but crucially also anchors the explanation to biological features, yielding more faithful rationales than using gene lists alone. While overall accuracy still trails candidate-matching approaches, the generative setting enables richer outputs: models can articulate why a label was chosen, highlight relevant genes, and remain extensible to novel types outside a fixed ontology. Future work will explore strengthening this interpretive capacity (e.g., through multiple [BIO] tokens tied to specific pathways or gene modules) and scaling aligned projections to larger LLMs.

378  
379     True Label: CD14+ Monocytes  
380     Predicted Label: Based on the sorted expressed genes, the most likely immune cell subtype  
381     is CD14+ Monocytes. The presence of genes such as TYROBP (DAP12), FCER1G (Fcgr1), ITGB2  
382     (CD29), and ITGAM (CD11b) suggests a monocytic lineage. [...skip] The absence of B cell-  
383     specific genes and T cell receptor genes (TR genes) further supports this conclusion.  
384  
385

383  
384     Figure 3: Example generative annotation on PBMC10K: BIOVERSE produces the label and reasoning  
385     grounded in gene evidence.

386  
387     Table 2: Molecular description generation results. S1: projection-only. S2: projection+LoRA

Model	BioFM	S1	S2	LLM-J	BERT-S	ROUGE-L
BIOVERSE	MAMMAL	30k	30k	<b>0.17</b>	<b>0.92</b>	<b>0.20</b>
		30k	–	0.10	0.92	0.18
BIOVERSE	ChemBERTa	130k	–	0.10	0.91	0.18
		30k	–	0.08	0.90	0.16
Granite-8B				0.04	0.91	0.07
LLaMA-70B				0.05	0.90	0.06
Mixtral-8x7B		(not applicable)		0.05	0.91	0.08
GPT-OSS-120B				0.02	0.89	0.06

### 397     5.2.2 MOLECULE DESCRIPTION GENERATION

398  
399     The molecular description generation task in Mol-Instructions (Fang et al., 2023) evaluates a model’s  
400     ability to produce detailed free-text descriptions of molecules given their SMILES representation.  
401     Target outputs cover structural features, physicochemical properties, biological activities, and potential  
402     applications, requiring the model to bridge symbolic chemical notation with natural language. We  
403     compare BIOVERSE with open-weight LLMs ranging from 8B (the same size as the BIOVERSE  
404     backbone) to 120B, all without BioFM alignment and therefore relying only on raw tokenized  
405     SMILES strings. We also test on the effect of using different BioFMs (ChemBERTa vs. MAMMAL)  
406     to generate the initial molecular embeddings. This tests whether BIOVERSE can flexibly adapt  
407     to modality-specific encoders without losing stability. All evaluations are conducted in a *zero-shot*  
408     *transfer* setting: Mol-Instructions descriptions are not used during alignment. Instead, BIOVERSE  
409     is aligned on independent molecule–text pairs from LLASmol (Yu et al., 2024), as described in  
410     Section 4.2.1. Table 2 shows BIOVERSE outperform open-domain LLMs significantly, regardless  
411     of the size. Switching from MAMMAL to ChemBERTa yields slightly worse results under the  
412     same training iterations, indicating that the framework is plug-and-play and stable across different  
413     molecular encoders. Additionally, the two-stage strategy (S1 followed by S2) is more effective than  
414     simply training S1 for longer. All three evaluation metrics show a consistent trend across our tests.  
415     We consider LLM-J to be the most meaningful metric for free-text generation; we therefore report  
416     only this metric in subsequent results.

### 416     5.2.3 PROTEIN-ORIENTED TEXT GENERATION

417  
418     We evaluate all four protein-oriented text generation benchmarks from Mol-Instructions (Fang et al.,  
419     2023): (1) catalytic activity prediction, (2) domain/motif prediction, (3) functional description  
420     generation, and (4) protein function prediction. Each task provides a protein sequence as input, and  
421     the model must generate free-text outputs describing a specific property of that sequence. Together,  
422     these tasks probe both factual grounding (e.g., motif recognition) and open-ended description ability,  
423     testing whether the model can jointly reason over the protein sequence and the accompanying prompt.

424  
425     Similar to the molecular task, we compare BIOVERSE with open-weight LLMs without BioFM  
426     alignment and therefore relying only on raw tokenized amino-acid sequences. We also conduct  
427     self-comparisons along two axes: (1) training iterations and (2) alignment strategies. As shown in  
428     Table 3, across all four tasks, BIOVERSE consistently outperforms open-domain LLMs by a wide  
429     margin. Longer alignment training further improves results, and the two-stage strategy, i.e., first  
430     training the projection (S1), then training projection and LoRA jointly (S2), yields the strongest  
431     performance. For instance, (30K S1 + 30K S2) outperforms (100K S1), and (100K S1 + 100K  
432     S2) outperforms (500K S1) in one task and achieved comparable overall scores in our benchmarks.  
433     Switching from MAMMAL (458M parameters) to a small ESM2 (8M parameters), the performance

432

433

Table 3: Protein text generation tasks results. All scores are LLM-J

434

435

Model	BioFM	Align.	S1	S2	catal.	motif	func.	prot.	Avg.
BIOVERSE	MAMMAL	AR	500k	500k	<b>0.37</b>	<b>0.21</b>	<b>0.40</b>	0.35	<b>0.33</b>
			100k	100k	0.35	0.19	0.38	0.32	0.31
			30k	30k	0.32	0.18	0.33	0.29	0.28
BIOVERSE	MAMMAL	AR	500k	–	0.34	0.20	0.38	0.38	0.32
			100k	–	0.26	0.17	0.33	0.32	0.27
			30k	–	0.21	0.11	0.22	0.31	0.21
BIOVERSE	MAMMAL	CT	30k	30k	0.33	<b>0.21</b>	0.39	<b>0.40</b>	<b>0.33</b>
			30k	–	0.00	0.01	0.01	0.00	0.01
BIOVERSE	ESM2-8M	AR	100k	–	0.21	0.12	0.20	0.24	0.19
Granite-8B					0.00	0.03	0.05	0.05	0.03
Mixtral-8x7B					0.00	0.02	0.06	0.02	0.02
LLaMA-70B				(not applicable)		0.01	0.03	0.09	0.05
GPT-OSS-120B						0.03	0.09	0.06	0.10

446

dropped, highlighting the impact of the encoder’s quality. When CT is used to reduce the training time in S1, it is important to follow it with S2, as S1-only does not teach the LLM backbone how to use those tokens in a generative task, and when combined with a prompt results in unexpected generation. However, a small S2 quickly bring up the performance of CT and with 30K S2 the performance is comparable to the longest run with AR. All results are reported in a zero-shot transfer setting. BIOVERSE is aligned (both S1 and S2) only on UniProtKB protein-text pairs with short GO terms and curated annotations, while evaluation is performed on the Mol-Instructions test split, which requires long-form, free-text property descriptions. This ensures that performance reflects transfer beyond the ontology terms used during alignment.

456

457

## 6 DISCUSSION AND FUTURE WORK

458

459

BIOVERSE demonstrates that BioFMs and LLMs can be aligned through lightweight projection layers, enabling generative reasoning across scRNA-seq, protein, and molecular modalities. This modular design allows compact LLMs to outperform much larger text-only baselines while producing richer, more interpretable outputs than candidate-matching approaches. By treating biological embeddings as first-class tokens, BIOVERSE bridges raw data and language-based reasoning in a way that is both scalable and deployable.

465

A key strength of BIOVERSE is its scalability across modalities: once aligned, scRNA-seq, proteins, and molecules can interoperate within the same LLM, supporting queries that span multiple levels of biology (e.g., “how does this variant protein affect cell type identity?” or “does this small molecule bind to this protein?”). Nonetheless, several limitations remain. The quality of alignment depends heavily on the underlying encoders, and modalities such as spatial transcriptomics or molecular 3D geometry are not yet explored. Current paired datasets rely largely on curated ontologies (e.g., GO terms, CellxGene metadata), which may bias reasoning and constrain coverage.

472

Looking ahead, several extensions are especially promising. First, interpretability can be enhanced by moving beyond single-token representations: gene-level, pathway-level, or topic-model embeddings (e.g., scETM (Zhao et al., 2021), cisTopic (Bravo González-Blas et al., 2019)) would yield more fine-grained rationales directly grounded in experimental data. Second, scaling to larger backbones (e.g., GPT-OSS-120B) and incorporating additional modalities such as epigenomics or spatial assays will test the limits of modularity and broaden biomedical applications. Third, standardized benchmarks are needed to evaluate not only accuracy but also interpretability, robustness, and factual grounding; multi-modal biological QA datasets remain scarce. Finally, integration into agentic workflows and privacy-preserving settings will be critical for real-world adoption. The design space is vast, and we have explored only a subset of configurations; further systematic ablations are essential. To accelerate progress, we will open-source our code and invite the community to co-develop multi-modal benchmarks and advance embedding-aware biomedical reasoning.

484

485

In summary, BIOVERSE offers a unified and extensible framework for embedding-aware biomedical reasoning, laying the groundwork for practical systems that connect raw scientific data with natural language understanding and interactive discovery.

486 REFERENCES  
487

488 Jean-Baptiste Alayrac, Jeff Donahue, Pauline Luc, Antoine Miech, Iain Barr, Yana Hasson, Karel  
489 Lenc, Arthur Mensch, Katherine Millican, Malcolm Reynolds, et al. Flamingo: a visual language  
490 model for few-shot learning. *Advances in neural information processing systems*, 35:23716–23736,  
491 2022.

492 Peter Belcak, Greg Heinrich, Shizhe Diao, Yonggan Fu, Xin Dong, Saurav Muralidharan, Yingyan Ce-  
493 line Lin, and Pavlo Molchanov. Small language models are the future of agentic ai. *arXiv preprint*  
494 *arXiv:2506.02153*, 2025.

495

496 Haiyang Bian, Yixin Chen, Xiaomin Dong, Chen Li, Minsheng Hao, Sijie Chen, Jinyi Hu, Maosong  
497 Sun, Lei Wei, and Xuegong Zhang. scmulan: a multitask generative pre-trained language model  
498 for single-cell analysis. In *International Conference on Research in Computational Molecular  
499 Biology*, pp. 479–482. Springer, 2024.

500 Nadav Brandes, Dan Ofer, Yam Peleg, Nadav Rappoport, and Michal Linial. Proteinbert: a universal  
501 deep-learning model of protein sequence and function. *Bioinformatics*, 38(8):2102–2110, 2022.

502

503 Carmen Bravo González-Blas, Liesbeth Minnoye, Dafni Papasokrati, Sara Aibar, Gert Hulselmans,  
504 Valerie Christiaens, Kristofer Davie, Jasper Wouters, and Stein Aerts. cistopic: cis-regulatory topic  
505 modeling on single-cell atac-seq data. *Nature methods*, 16(5):397–400, 2019.

506

507 Yiqun Chen and James Zou. Genept: a simple but effective foundation model for genes and cells  
508 built from chatgpt. *bioRxiv*, pp. 2023–10, 2024.

509

510 Seyone Chithrananda, Gabriel Grand, and Bharath Ramsundar. Chemberta: large-scale self-  
511 supervised pretraining for molecular property prediction. *arXiv preprint arXiv:2010.09885*, 2020.

512

513 Hongyoon Choi, Jeongbin Park, Sumin Kim, Jiwon Kim, Dongjoo Lee, Sungwoo Bae, Haenara Shin,  
514 and Daeseung Lee. Cellama: foundation model for single cell and spatial transcriptomics by cell  
embedding leveraging language model abilities. *bioRxiv*, pp. 2024–05, 2024.

515

516 Haotian Cui, Chloe Wang, Hassaan Maan, Kuan Pang, Fengning Luo, Nan Duan, and Bo Wang.  
517 scgpt: toward building a foundation model for single-cell multi-omics using generative ai. *Nature  
518 methods*, 21(8):1470–1480, 2024.

519

520 Bharath Dandala, Michael M Danziger, Ella Barkan, Tanwi Biswas, Viatcheslav Gurev, Jianying  
521 Hu, Matthew Madgwick, Akira Koseki, Tal Kozlovska, Michal Rosen-Zvi, et al. Bmfm-rna: An  
522 open framework for building and evaluating transcriptomic foundation models. *arXiv preprint*  
523 *arXiv:2506.14861*, 2025.

524

525 Yin Fang, Xiaozhuan Liang, Ningyu Zhang, Kangwei Liu, Rui Huang, Zhuo Chen, Xiaohui Fan, and  
526 Huajun Chen. Mol-instructions: A large-scale biomolecular instruction dataset for large language  
527 models. *arXiv preprint arXiv:2306.08018*, 2023.

528

529 Adam Gayoso, Romain Lopez, Galen Xing, Pierre Boyeau, Valeh Valiollah Pour Amiri, Justin Hong,  
530 Katherine Wu, Michael Jayasuriya, Edouard Mehlman, Maxime Langevin, et al. A python library  
531 for probabilistic analysis of single-cell omics data. *Nature biotechnology*, 40(2):163–166, 2022.

532

533 John Jumper, Richard Evans, Alexander Pritzel, Tim Green, Michael Figurnov, Olaf Ronneberger,  
534 Kathryn Tunyasuvunakool, Russ Bates, Augustin Žídek, Anna Potapenko, et al. Highly accurate  
535 protein structure prediction with alphafold. *nature*, 596(7873):583–589, 2021.

536

537 Jinhyuk Lee, Wonjin Yoon, Sungdong Kim, Donghyeon Kim, Sunkyu Kim, Chan Ho So, and Jaewoo  
538 Kang. Biobert: a pre-trained biomedical language representation model for biomedical text mining.  
539 *Bioinformatics*, 36(4):1234–1240, 2020.

540

541 Junnan Li, Dongxu Li, Silvio Savarese, and Steven Hoi. Blip-2: Bootstrapping language-image  
542 pre-training with frozen image encoders and large language models. In *International conference  
543 on machine learning*, pp. 19730–19742. PMLR, 2023.

540 Zeming Lin, Halil Akin, Roshan Rao, Brian Hie, Zhongkai Zhu, Wenting Lu, Nikita Smetanin,  
 541 Robert Verkuil, Ori Kabeli, Yaniv Shmueli, et al. Evolutionary-scale prediction of atomic-level  
 542 protein structure with a language model. *Science*, 379(6637):1123–1130, 2023.

543

544 Haotian Liu, Chunyuan Li, Qingyang Wu, and Yong Jae Lee. Visual instruction tuning. *Advances in*  
 545 *neural information processing systems*, 36:34892–34916, 2023a.

546 Tianyu Liu, Kexing Li, Yuge Wang, Hongyu Li, and Hongyu Zhao. Evaluating the utilities of  
 547 foundation models in single-cell data analysis. *bioRxiv*, pp. 2023–09, 2023b.

548

549 Qizhi Pei, Wei Zhang, Jinhua Zhu, Kehan Wu, Kaiyuan Gao, Lijun Wu, Yingce Xia, and Rui Yan.  
 550 Biot5: Enriching cross-modal integration in biology with chemical knowledge and natural language  
 551 associations. *arXiv preprint arXiv:2310.07276*, 2023.

552 Jeffrey M. Perkel. 85 million cells — and counting — at your fingertips. *Nature*, 629:248–249,  
 553 2024. doi: 10.1038/d41586-024-01217-y. URL <https://www.nature.com/articles/d41586-024-01217-y>.

555

556 Alec Radford, Jong Wook Kim, Chris Hallacy, Aditya Ramesh, Gabriel Goh, Sandhini Agarwal,  
 557 Girish Sastry, Amanda Askell, Pamela Mishkin, Jack Clark, et al. Learning transferable visual  
 558 models from natural language supervision. In *International conference on machine learning*, pp.  
 559 8748–8763. PMLR, 2021.

560

561 Jerret Ross, Brian Belgodere, Vijil Chenthamarakshan, Inkit Padhi, Youssef Mroueh, and Payel Das.  
 562 Large-scale chemical language representations capture molecular structure and properties. *Nature*  
 563 *Machine Intelligence*, 4(12):1256–1264, 2022.

564

565 Moritz Schaefer, Peter Peneder, Daniel Malzl, Mihaela Peycheva, Jake Burton, Anna Hakobyan,  
 566 Varun Sharma, Thomas Krausgruber, Joerg Menche, Eleni M Tomazou, et al. Multimodal learning  
 567 of transcriptomes and text enables interactive single-cell rna-seq data exploration with natural-  
 568 language chats. *bioRxiv*, pp. 2024–10, 2024.

569

570 Yaorui Shi, Jiaqi Yang, Changhao Nai, Sihang Li, Junfeng Fang, Xiang Wang, Zhiyuan Liu, and  
 571 Yang Zhang. Language-enhanced representation learning for single-cell transcriptomics. *arXiv*  
 572 *preprint arXiv:2503.09427*, 2025.

573

574 Yoel Shoshan, Moshiko Raboh, Michal Ozery-Flato, Vadim Ratner, Alex Golts, Jeffrey K Weber, Ella  
 575 Barkan, Simona Rabinovici-Cohen, Sagi Polaczek, Ido Amos, et al. Mammal–molecular aligned  
 576 multi-modal architecture and language. *arXiv preprint arXiv:2410.22367*, 2024.

577

578 Ross Taylor, Marcin Kardas, Guillem Cucurull, Thomas Scialom, Anthony Hartshorn, Elvis Saravia,  
 579 Andrew Poultton, Viktor Kerkez, and Robert Stojnic. Galactica: A large language model for science.  
 580 *arXiv preprint arXiv:2211.09085*, 2022.

581

582 Christina V Theodoris, Ling Xiao, Anant Chopra, Mark D Chaffin, Zeina R Al Sayed, Matthew C  
 583 Hill, Helene Mantineo, Elizabeth M Brydon, Zexian Zeng, X Shirley Liu, et al. Transfer learning  
 584 enables predictions in network biology. *Nature*, 618(7965):616–624, 2023.

585

586 Eric Wang, Samuel Schmidgall, Paul F Jaeger, Fan Zhang, Rory Pilgrim, Yossi Matias, Joelle Barral,  
 587 David Fleet, and Shekoofeh Azizi. Txgemma: Efficient and agentic llms for therapeutics. *arXiv*  
 588 *preprint arXiv:2504.06196*, 2025a.

589

590 Weiyun Wang, Zhangwei Gao, Lixin Gu, Hengjun Pu, Long Cui, Xingguang Wei, Zhaoyang Liu,  
 591 Linglin Jing, Shenglong Ye, Jie Shao, et al. Internv13. 5: Advancing open-source multimodal  
 592 models in versatility, reasoning, and efficiency. *arXiv preprint arXiv:2508.18265*, 2025b.

593

594 Fan Yang, Wenchuan Wang, Fang Wang, Yuan Fang, Duyu Tang, Junzhou Huang, Hui Lu, and  
 595 Jianhua Yao. scbert as a large-scale pretrained deep language model for cell type annotation of  
 596 single-cell rna-seq data. *Nature Machine Intelligence*, 4(10):852–866, 2022.

597

598 Botao Yu, Frazier N Baker, Ziqi Chen, Xia Ning, and Huan Sun. Llasmol: Advancing large language  
 599 models for chemistry with a large-scale, comprehensive, high-quality instruction tuning dataset.  
 600 *arXiv preprint arXiv:2402.09391*, 2024.

594 Xinyu Yuan, Zhihao Zhan, Zuobai Zhang, Manqi Zhou, Jianan Zhao, Boyu Han, Yue Li, and Jian  
 595 Tang. Cell ontology guided transcriptome foundation model. *Advances in Neural Information  
 596 Processing Systems*, 37:6323–6366, 2024.

597 Suyuan Zhao, Jiahuan Zhang, Yushuai Wu, Yizhen Luo, and Zaiqing Nie. Langcell: Language-cell  
 598 pre-training for cell identity understanding. *arXiv preprint arXiv:2405.06708*, 2024.

600 Yifan Zhao, Huiyu Cai, Zuobai Zhang, Jian Tang, and Yue Li. Learning interpretable cellular and  
 601 gene signature embeddings from single-cell transcriptomic data. *Nature communications*, 12(1):  
 602 5261, 2021.

## 604 A APPENDIX

### 606 A.1 EVALUATION METRICS

608 We evaluate generative tasks using three complementary metrics.

610 **LLM-as-a-Judge** We use single-output, reference-based evaluation prompt (see below), where each  
 611 model response is scored independently against the expected output. Each evaluation is repeated with  
 612 3 different random seeds (temperature = 0.2), and the average similarity score is reported.

613 **BERTScore** We compute semantic similarity using BERTScore with PubMedBERT embeddings,  
 614 which is robust to paraphrasing and biomedical terminology variation.

615 **ROUGE-L** As a legacy baseline, we report ROUGE-L  $F_1$  (with stemming), which measures longest  
 616 common subsequence overlap between candidate and reference.

617 This combination captures factual correctness and coverage (LLM-Judge), semantic similarity  
 618 (BERTScore), and surface-form overlap (ROUGE-L).

### 620 A.2 PUBLIC OPEN-WEIGHTS MODELS

622 We list the public open-weight language models used in our experiments:

- 624 • **GPT-OSS-120B:** An open-weight, text-only model by OpenAI, available under the Apache  
 625 2.0 license. Designed for reasoning and agentic tasks.  
 626 GitHub: <https://github.com/openai/gpt-oss>  
 627 HuggingFace: <https://huggingface.co/openai/gpt-oss-120b>
- 628 • **Granite-8B:** We use granite-3.3-8b-instruct, available under the Apache 2.0  
 629 license.  
 630 GitHub: [https://github.com/ibm-granite/granite-3.  
 631 3-language-models](https://github.com/ibm-granite/granite-3.3-language-models)  
 632 HuggingFace: [https://huggingface.co/ibm-granite/granite-3.  
 633 3-8b-instruct](https://huggingface.co/ibm-granite/granite-3.3-8b-instruct)
- 634 • **LLaMA-70B:** Meta’s open-weight large language model (Llama-3.3-70B-Instruct),  
 635 available under a community license. Widely used for research and instruction-tuned  
 636 variants.  
 637 GitHub: <https://github.com/meta-llama/llama>  
 638 HuggingFace: [https://huggingface.co/meta-llama/Llama-3.  
 639 3-70B-Instruct](https://huggingface.co/meta-llama/Llama-3.3-70B-Instruct)
- 640 • **Mixtral-8x7B:** A mixture-of-experts open-weight model released by Mistral AI, featuring 8  
 641 experts with 2 active per token. Available under the Apache 2.0 license.  
 642 GitHub: <https://github.com/mistralai/mistral-inference>  
 643 HuggingFace: [https://huggingface.co/mistralai/  
 644 Mixtral-8x7B-Instruct-v0.1](https://huggingface.co/mistralai/Mixtral-8x7B-Instruct-v0.1)

### 645 A.3 TRAINING DETAILS

646 All experiments were conducted using the hyperparameters and configuration settings detailed below,  
 647 extracted from our training scripts.

648     A.3.1 MODEL & ARCHITECTURE  
 649  
 650     • **Base LLM:** ibm-granite/granite-3.3-8b-instruct  
 651  
 652     • **Adapter Method:** Low-Rank Adaptation (LoRA) was enabled for stage-2.  
 653  
 654     • **Input Embedding Model:** mammal  
 655  
 656  
 657     A.3.2 LoRA CONFIGURATION  
 658  
 659     • **Rank (r):** 16  
 660  
 661     • **Alpha (lora\_alpha):** 32  
 662  
 663     • **Dropout (lora\_dropout):** 0.05  
 664  
 665     • **Target Modules:** All linear layers (all-linear)  
 666  
 667     • **Bias:** none  
 668  
 669     • **Task Type:** Causal Language Modeling (CAUSAL\_LM)  
 670  
 671  
 672  
 673     A.3.3 TRAINING HYPERPARAMETERS  
 674  
 675     • **Optimizer:** AdamW (Hugging Face Trainer default)  
 676  
 677     • **Learning Rate:**  $2 \times 10^{-5}$   
 678  
 679     • **LR Scheduler:** Linear warmup for 100 steps, then cosine decay.  
 680  
 681  
 682     • **Weight Decay:** 0.01  
 683  
 684     • **Batch Size:** 4 per device  
 685  
 686  
 687     • **Gradient Accumulation Steps:** 1  
 688  
 689     • **Max Gradient Norm:** 1.0  
 690  
 691     • **Precision:** Mixed-precision using bf16  
 692  
 693     • **Seed:** 1234  
 694  
 695     • **Maximum Training Steps:** 10,000  
 696  
 697  
 698     • **Evaluation Frequency:** Every 100 steps  
 699  
 700

701     Experiments were run on a node with 2 NVIDIA A100 GPUs using PyTorch 2.2 and the Hugging  
 Face Transformers library.

702 A.4 PROMPTS

703

## 704 A.4.1 LLM-AS-A-JUDGE PROMPT

705

706 You are an expert evaluator tasked with assessing the quality of a model's response to  
 707 a given instruction and input. Your goal is to compare the model's response to the  
 708 expected output and provide a similarity score between 0 and 1, where:  
 709 - 0 means the response is completely unrelated or incorrect.  
 709 - 1 means the response is perfectly aligned with the expected output.

710

710 Consider the following aspects when evaluating:

711

1. **Instruction Adherence**: Does the response correctly follow the instruction?
2. **Input Relevance**: Does the response appropriately use the provided input?
3. **Semantic Similarity**: Does the response convey the same meaning as the expected output?
4. **Accuracy**: Are the facts or details in the response correct and consistent with the expected output?
5. **Completeness**: Does the response include all key information from the expected output?

712

712 Score Guidelines:

713

713 Use the following scale to assign a similarity score:

714

- 0.00 Completely unrelated, off-topic, or incorrect.
- 0.25 Minimal relevance or correctness; major elements are missing or wrong.
- 0.50 Some relevant aspects present but key points are missing or inaccurate.
- 0.75 Highly similar; closely matches the expected output with minor omissions or differences.
- 1.00 Perfect match in meaning, accuracy, and completeness.

715

715 Instruction:

716

716 {instruction}

717

717 Input:

718

718 {input}

719

719 Model's Response:

720

720 {response}

721

721 Expected Output:

722

722 {expected\_output}

723

723 Output Format (JSON):

724

724 {  
 725     "similarity\_score": <float>,  
 726     "explanation": <string>  
 727 }

728

729

## 730 A.4.2 CELL TYPE ANNOTATION INSTRUCTION-CONSTRAINED PROMPT

731

732 You are an expert cell biologist. Given the following information, predict the most  
 733 likely immune cell subtype. You MUST only choose from the following list of possible  
 734 cell types:

735

735 "B cells",  
 736 "CD14+ Monocytes",  
 737 "CD4 T cells",  
 738 "CD8 T cells",  
 739 "Dendritic Cells",  
 740 "FCGR3A+ Monocytes",  
 741 "Megakaryocytes",  
 742 "NK cells",  
 743 "Other"

744

744 Sorted expressed genes (most abundant first, top 128): {genes\_str}  
 745 Cell embedding: [BIO]

746

746 Please respond with exactly one cell type from the list above,  
 747 with reasoning of your choice.

748

749

750

751

752

753

## 754 A.5 CODE AND DATA

755

755 Code will be released upon acceptance. For anonymized review, we provide simplified code in  
 756 Jupyter notebook format and a description of datasets.

756  
757

## A.6 USE OF LARGE LANGUAGE MODELS (LLMs)

758  
759  
760  
761  
762  
763

We acknowledge the use of large language models (LLMs) to assist in the preparation of this manuscript. The LLM was utilized for three primary purposes: (1) aiding in literature discovery to identify recent and relevant publications, (2) assisting with the formatting of LaTeX syntax for tables and equations, and (3) rephrasing sentences to improve clarity and readability. All information, including citations and scientific claims, was verified by the authors, who take full responsibility for the final content of this paper.

764  
765  
766  
767  
768  
769  
770  
771  
772  
773  
774  
775  
776  
777  
778  
779  
780  
781  
782  
783  
784  
785  
786  
787  
788  
789  
790  
791  
792  
793  
794  
795  
796  
797  
798  
799  
800  
801  
802  
803  
804  
805  
806  
807  
808  
809